# Low ion-velocity slowing down in a strongly magnetized plasma target

Claude Deutsch[*] and Romain Popoff

*LPGP (UMR-CNRS 8578), Université Paris XI, 91405 Orsay, France*

(Received 28 August 2008; published 19 November 2008)

An ion projectile stopping at a velocity smaller than the target electron thermal velocity in a strong magnetic field is investigated within a different diffusion formulation, based on Green-Kubo integrands evaluated in magnetized one component plasma models, respectively framed on target ions and electrons. Analytic expressions are reported for slowing down orthogonal and parallel to an arbitrary large magnetic field, which are free from the usual uncertainties plaguing the standard perturbative derivations. Magnetic and target temperature dependences of the low velocity slowing down are thoroughly detailed for dense plasmas of fast ignition concern and ultracold plasmas envisioned for ion beam cooling, as well.

## I. INTRODUCTION AND MOTIVATION

Ion beam stopping in a dense plasma submitted to an arbitrary large and steady magnetic field **B** is a recurrent topic encompassing a huge range of practical situations of very high interest. This range includes ultracold plasmas (UCPs) [1], cold electron setups used for ion beam cooling [2–4], as well as many very dense systems involved in magnetized target fusions (MTFs) [5], or inertial confinement fusion (ICF). This latter thermonuclear scheme presently advocates a highly regarded fast ignition scenario (FIS) [6], based on femtolaser produced proton or heavier ion beams impinging a precompressed capsule containing a thermonuclear fuel [7] in it. Then, *B* values up to $10^{10}$ G may be reached in the laboratory [8]. Such a topic is also of intense astrophysical concern [9]. These interaction geometries highlight low ion velocity slowing down (LIVSD) as playing a fundamental role in asserting the confining capabilities and thermonuclear burn efficiency in dense and strongly magnetized media.

Up to now, the basic features of ion stopping in a dense and arbitrary magnetized plasma have been essentially approached through a twofold methodology. The latter mostly elaborates on a clever combination of the binary collision (BC) method with the linear response (LR) highlighting a collective dielectric description of the target electron fluid. This combination is now perfectly well mastered in the absence of an applied magnetic field (*B*=0). It keeps its efficiency when $B \neq 0$, by emulating short and large distance cutoffs with a replacement of the base Coulomb interaction by a renormalized one including diffraction corrections ($\eta \neq 0$) at short distances and Debye screening at large ones [2,23].

However, very significant gaps in this program involve the crucial ion stopping along **B** and perpendicular to it. In particular, at high *B* values, the BC predicts a vanishingly parallel energy loss, which remains at variance with the nonzero LR one.

Also challenging BC-LR discrepancies persist in the orthogonal direction, especially for vanishingly small ion projectile velocity $V_b \rightarrow 0$.

Quantitatively, the reliability of the BC-LR combination is mostly grounded on a good agreement with numerical simulations out of a classical trajectory Monte Carlo (CTMC) code. However, this code exhibits too high a level of numerical noise at large *B* values, and in the $V_b \rightarrow 0$ limit, while keeping a plasma coupling below unity, which is precisely the domain of many important applications of current interest, as those envisioned in the sequel, This situation motivates us to propose an alternative approach to this parameter range, by implementing low ion velocity slowing down (LIVSD) through diffusion coefficients of the magnetized one component plasma featuring either the target electrons or target ions.

As detailed below, these methods allow for a direct and complete accounting of the low frequency plasma modes involved in the LIVSD mechanism, in the presence of an arbitrary strong magnetic field.

Our present goal is to demonstrate that transverse and parallel LIVSD to **B** may be given analytic expressions through a derivation free from ambiguities usually plaguing the most sophisticated combination of binary collision approximation and dielectric response [2–4]. We thus implement a radically different approach [10] to LIVSD when projectile velocity $V_b$ remains smaller than target electron thermal velocity $V_{the}$. We thus consider ion stopping,

$$S(V_b) \equiv \frac{dE_b}{dx}(V_b), \tag{1}$$

near $V_b=0$. The ratio $S(V_b)/V_b$ usually monitors a linear stopping profile, up to 100 keV/amu [11] in cold matter. Similar trends are also reported in highly ionized plasma with B=0 [12] or $B \neq 0$ [2].

From now on, we intend to make use of a very powerful connection between very low velocity ion stopping and particle diffusion through Einstein characterization of ion mobility associated to thermal electron fluctuations in target, around the slow ion projectile visualized as an impurity immersed in a dense and homogeneous electron fluid. Technically, we are then led to use the recently proposed and exact Dufty-Berkovsky relationship [11,13]

———
*Corresponding author. FAX: 331 69 15 78 44. claude.deutsch@u-psud.fr

$$\lim_{V_{\mathrm{b}}\to 0}\frac{S(V_{\mathrm{b}})}{V_{\mathrm{b}}}=k_{\mathrm{B}}T_{\mathrm{e}}D^{-1}, \tag{2}$$

connecting the ratio of stopping to $V_b$ in the zero velocity limit with the ion diffusion coefficient in target.

We first detail the determination of $D$ in a framework of magnetized one-component-plasmas (OCP) models through specific magnetohydrodynamic modes. Then, we check the implementation of Eq. (2) in the zero field ($B=0$) case. We display typical LIVSD $B$ and $T$ behaviors for a dense target of ICF concern [6–8], and an ultracold plasma of ion beam cooling interest [2–4]. We stress transverse and parallel geometries

## II. FORMALISM

### A. General

In a magnetized plasma the particle self-diffusion coefficient $D$ can be readily expressed in terms of Green-Kubo integrands (GKIs) involving field fluctuations in the target electron fluid, under the form

$$D=\frac{c^2}{B^2}\int_0^\infty d\tau\langle\vec{E}(\tau)\cdot\vec{E}(0)\rangle \tag{3}$$

in terms of an equilibrium canonical average of the two-point autocorrelation function for fluctuating electric fields [14,15].

At this juncture we need to frame the GKI in suitable magnetized one component plasma (OCP) models [14,15] for the transverse and parallel geometries, respectively. This procedure implies that the slowly incoming ions are evolving against a background of faster fluctuating target electrons ($V_{\mathrm{b}}<V_{\mathrm{the}}$) providing the OCP rigid neutralizing background thus validating the OCP assumption.

Moreover, restricting to proton projectiles impacting an electron-proton plasma [16], we immediately perceive the pertinence of the diffusion-based LIVSD as phrased by Eq. (2).

First, the proton beam can easily self-diffuse amongst its target homologues, while the same mechanism experienced by target electrons allow them to drag ambipolarly the incoming proton projectiles [17]. So, the transverse electron LIVSD can be either monitored by the well known classical diffusion $D_\perp \sim B^{-2}$, or by the Bohmlike hydrodynamic one with $D_\perp \sim B^{-1}$. In the first case, momentum conservation at the level of the electron-ion pair implies that the ions will diffuse with the same coefficient as the electrons. Finally, we should also notice that the relationship (2) implies the existence of *bona fide* diffusion coefficients, through a nonzero minimum for the electron collision frequency.

Transverse $D_\perp$ and parallel $D_\parallel$ diffusion coefficient have already been discussed at length by Marchetti *et al.* [14] and Cohen-Suttorp [15]. Their derivation is based on the specific features of four finite frequency and propagating hydromodes in a strongly magnetized OCP with the ratio of plasma to cyclotron frequencies, $\omega_{\mathrm{p}}/\omega_{\mathrm{b}}<1$.

### B. MHD OCP modes

According to the Marchetti-Kirkpatrick-Dorfman (MKD) analysis [14] there are five modes: four propagating finite frequency modes and one purely diffusive mode. They are as follows:

(i) Two high-frequency modes, known in the Vlasov limit as the first Bernstein modes, or the upper hybrid modes. The dispersion relation is given for $\omega_{\mathrm{p}}/\omega_{\mathrm{b}}\ll 1$ by

$$\omega_{h\sigma}(\mathbf{k})=i\sigma\omega_{\mathrm{b}}\left(1+\frac{1}{2}\frac{\omega_{\mathrm{p}}^2}{\omega_{\mathrm{b}}^2}\hat{k}_\perp^2+\frac{\gamma}{2\rho\chi_{\mathrm{T}}}\frac{k_\perp^2}{\omega_{\mathrm{b}}^2}\right)$$
$$+k_z^2\nu_\parallel(i\sigma\omega_{\mathrm{b}})\left(1+\frac{1}{2}\hat{k}_\perp^2\frac{\omega_{\mathrm{p}}^2}{\omega_{\mathrm{b}}^2}\right)$$
$$+k_\perp^2\nu_\perp(i\sigma\omega_{\mathrm{b}}|\hat{k}_z|)+0(k^3) \tag{4}$$

with $\sigma=\pm 1$. When $\mathbf{B}=\mathbf{0}$, these modes reduce to the plasma modes. $\gamma=c_p/c_v$ is the ratio of specific heats, $\rho=nm$ and $\chi_T$ is the isothermal compressibility.

(ii) Two finite-frequency modes, known in the Vlasov limit as the propagating plasma modes, with frequency, for $\omega_{\mathrm{p}}/\omega_{\mathrm{b}}\ll 1$,

$$\omega_{\nu\sigma}(\mathbf{k})=i\sigma\omega_{\mathrm{p}}|k_z|\left(1+\frac{\gamma}{2\rho\chi_{\mathrm{T}}}\frac{k^2}{\omega_{\mathrm{b}}^2}-\frac{1}{2}\hat{k}_\perp^2\frac{\omega_{\mathrm{p}}^2}{\omega_{\mathrm{b}}^2}-\frac{3\gamma}{4\rho\chi_{\mathrm{T}}}\frac{k_\perp^2}{\omega_{\mathrm{b}}^2}\right)$$
$$+k_z^2\nu_\parallel'(i\sigma\omega_{\mathrm{p}}|\hat{k}_z|)\left(1+\hat{k}_\perp^2\frac{\omega_{\mathrm{p}}^2}{\omega_{\mathrm{b}}^2}\right)$$
$$+k_\perp^2\nu_\perp'(i\sigma\omega_{\mathrm{p}}|\hat{k}_z|)+0(k^3). \tag{5}$$

When $\mathbf{B}=\mathbf{0}$, these reduce to then shear modes.

(iii) One diffusive heat mode, with dispersion relation

$$\omega_H(k)=D_\parallel^{\mathrm{T}}k_z^2+D_\perp^{\mathrm{T}}k_\perp^2+0(k^4) \tag{6}$$

which does contribute to particle transport, and is thus ignored in the sequel.

Here $\hat{k}_\perp=k_\perp/k$ and $\hat{k}_z=k_z/k$. In Eqs. (4) and (5) terms of $0(\omega_{\mathrm{p}}^3/\omega_{\mathrm{b}}^3)$ have been neglected.

The viscosities $\nu_\parallel$, $\nu_\perp$, $\nu_\parallel'$, and $\nu_\perp'$ are linear combinations of the five kinematic viscosities $\nu_j$ for $j=0,1,\ldots,4$. They are defined as

$$\nu_\parallel(i\sigma\omega_{\mathrm{b}})=\nu_2(i\sigma\omega_{\mathrm{b}})-i\sigma\nu_4(i\sigma\omega_{\mathrm{b}}), \tag{7a}$$

$$\nu_\perp(i\sigma\omega_{\mathrm{b}})=\nu_1(i\sigma\omega_{\mathrm{b}})+\frac{1}{6}\nu_0(i\sigma\omega_{\mathrm{b}})-i\sigma\nu_3(i\sigma\omega_{\mathrm{b}}) \tag{7b}$$

and

$$\nu_\parallel'(i\sigma\omega_{\mathrm{p}}|\hat{k}_z|)=\frac{2}{3}-\nu_0(i\sigma\omega_{\mathrm{p}}|\hat{k}_z|), \tag{7c}$$

$$\nu_\perp'(i\sigma\omega_{\mathrm{p}}|\hat{k}_z|)=\frac{1}{2}\nu_2(i\sigma\omega_{\mathrm{p}}|\hat{k}_z|)+i\sigma\frac{\omega_{\mathrm{p}}}{\omega_{\mathrm{b}}}|\hat{k}_z|\nu_4(i\sigma\omega_{\mathrm{p}}|\hat{k}_z|). \tag{7d}$$

As expected, they are finite frequency complex transport coefficients.

The viscosities are evaluated to lowest order in the plasma parameter for the propagating modes as

$$\nu_0^0(i\sigma\omega_p|\hat{k}_z|) = \frac{1}{m\beta}\left(\frac{2\nu_c}{5\sqrt{\pi}} - i\sigma\omega_p|\hat{k}_z|\right)^{-1},$$

$$\nu_1^0(i\sigma\omega_p|\hat{k}_z|) \cong \frac{1}{m\beta\omega_b^2}\frac{\nu_c}{10\sqrt{\pi}} - \frac{i\sigma\omega_p|\hat{k}_z|}{4m\beta\omega_b^2},$$

$$\nu_2^0(i\sigma\omega_p|\hat{k}_z|) \cong \frac{1}{m\beta\omega_b^2} - \frac{2\nu_c}{5\sqrt{\pi}} - \frac{i\sigma\omega_p|\hat{k}_z|}{m\beta\omega_b^2},$$

$$\nu_3^0(i\sigma\omega_p|\hat{k}_z|) \cong \frac{1}{2m\beta\omega_b},$$

$$\nu_4^0(i\sigma\omega_p|\hat{k}_z|) \cong \frac{1}{m\beta\omega_b}. \tag{8}$$

The imaginary parts of $\nu_3$ and $\nu_4$ are neglected because they are of order $(\omega_p/\omega_b)^3$.

The time evolution of the currents in the limit $\varepsilon_p < 1$ can be approximately described by the Landau kinetic equation. MKD find that $\nu_\parallel$, $\nu'_\parallel$, and $D_\parallel^T$ are $0(\omega_b^0)$; Re $\nu_\perp$, Re $\nu'_\perp$, and $D_\perp^T$ are $0(\omega_b^{-2})$; and Im $\nu_\perp$ as well as Im $\nu'_\perp$ are $0(\omega_b^{-1})$.

To leading order in $\omega_p/\omega_b$, the upper hybrid modes represent velocity fluctuations in the $xy$ plane, while the propagating plasma modes are associated with density fluctuations and fluctuations of velocity in the $z$ direction. The heat mode represents temperature and density fluctuations.

### C. Self-diffusion coefficients

So, exploring first the $\omega_b \gtrsim \omega_p$ domain, one can explicit the parallel and $B$ independent diffusion [14],

$$D_\parallel^{(0)} = \frac{3\sqrt{\pi}V_{thi}^2}{\nu_c} \sim 0(\omega_b^0), \tag{9a}$$

where $V_{thi}^2 = \frac{k_B T}{M_p}$, and $\nu_c = \omega_p\varepsilon_p \ln(1/\varepsilon_p)$ in terms of the plasma parameter $\varepsilon_p = 1/n\lambda_D^3$, where $n$ denotes charge particle density, and $\lambda_D$, the Debye length, in a beam plasma system taken as globally neutral with $\nu_c/\omega_b \ll 1$.

At the same level of approximation transverse diffusion reads as [14]

$$D_\perp^{(0)} = \frac{r_L^2\nu_c}{3\sqrt{\pi}} \sim 0(\omega_b^{-2}), \tag{9b}$$

in terms of Larmor radius $r_L = V_{thi}/\omega_b$.

With higher $B$ values ($\omega_b \gg \omega_p$) one reaches the transverse hydro-Bohm regime featuring [14,18]

$$D_\perp = D_\perp^{(0)} + \frac{0.5V_{thi}^2}{\omega_b}\varepsilon_p^2[\ln(1/\varepsilon_p)]^{3/2}, \tag{10}$$

while parallel diffusion retains a $\omega_b$ dependence through [13]

$$D_\parallel^{-1} = \frac{\Gamma^{5/2}}{\omega_p a^2}\left(\frac{3}{\pi}\right)^{1/2} \cdot \left(0.5\ln(1+X^2) - 0.3 + \frac{0.0235}{r^2}\right), \tag{11}$$

where

$$\Gamma = \frac{a^2}{3\lambda_D^2} \quad \text{with } a = \left(\frac{3}{4\pi n}\right)^{1/3}, \quad r = \frac{\omega_p}{\omega_b},$$

$$\text{and } X = \frac{1}{\sqrt{3}} \cdot \frac{1}{\Gamma^{3/2}}.$$

$\Gamma < 1$ encompasses, most if not all, situations of practical interest.

When electron diffusion is considered, $V_{the}$ should be used in Eq. (10), and the above ambipolar process has to be implemented.

### III. $B = 0$ LIMIT

In order to document the LIVSD physics highlighted by the Dufty-Berkovsky (DB) expression (2), we first pay attention to the unmagnetized $B = 0$ limit. We investigate it through three independent avenues. First, we consider the usual single projectile ion slowing down into the target electron fluid described in the small $\varepsilon_p$ limit as a Fried Conte dielectric [12,20,21] Then, low velocity ion stopping can be expressed under the form ($N_D = n\lambda_D^3$)

$$-\left|\frac{dE}{dx}\right| = R_1 v_P + R_3 v_p^3 + 0(v_p^5), \tag{12}$$

with the "friction coefficient"

$$R_1 = \frac{Z^2 N_D}{12\pi\sqrt{2\pi}}\left(\ln(K^2+1) - \frac{K^2}{K^2+1}\right), \tag{12a}$$

and the $v_p^3$ coefficient

$$R_3 = \frac{Z^2 N_D}{12\pi\sqrt{2\pi}}\left[-\frac{3}{10}\ln(K^2+1) + \left(\frac{8}{5} - \frac{\pi}{20}\right)\right.$$

$$-\frac{29}{10}\frac{1}{k^2+1} + \left(\frac{13}{10} + \frac{3\pi}{20}\right)$$

$$\left.\times\ \frac{1}{(K^2+1)^2} + \frac{\pi}{10}\frac{1}{(K^2+1)^3}\right], \tag{12b}$$

where $Z = Z/N_D$ and $K = 8\pi n\lambda_D^3/Z$. In the present $\varepsilon_p < 1$ approximation, we always witness $R_3 \ll R_1$, which validates quantitatively the exact DB result (2).

An obvious alternative to the series (12) is afforded through the $B = 0$ limit of the $B$-perturbative analysis worked out by Steinberg and Ortner [19], with

$$-\frac{dE}{dx} = \frac{2}{3}\frac{(2\pi m)^{1/2}}{(kT)^{3/2}}Z^2 e^4 nD V_p, \quad m = \text{electron mass}, \tag{13}$$

and $D = -\ln(y^2/8) - C - 1$, where $y = \hbar\omega_p/kT$ and $C = 0.5722$, denotes the Euler constant.

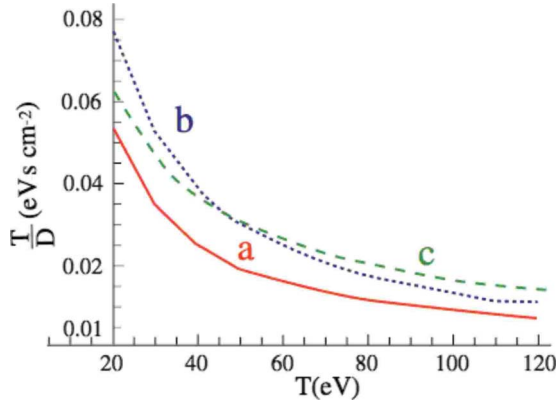FIG. 1. (Color online) Low velocity proton stopping in dense plasma ($n=10^{21}$ $e$-cm$^{-3}$) in terms of target temperature, (a) $B=0$, LIVSD, Eqs. (12) and (13), (b) $B=0$, LIVSD, Eq. (14), and (c) parallel LIVSD, Eq. (2) with Eq. (9a).

Expressions (12) and (13) are quantitatively equivalent, thus providing a theoretical template against which to evaluate LIVSD deduced from OCP diffusion coefficients.

The second advocated route implements the small $\varepsilon_p$ approximation for that $B=0$ self-diffusion coefficient given by Sjögren *et al.* [22], under the form

$$D_2 = \frac{104Z^2 + 111\sqrt{2}Z + 59}{32Z^2 + 75\sqrt{2}Z + 50}D_2^{(1)}, \quad (14)$$

with

$$D_2^{(1)} = a^2\omega_p\left(\frac{\pi}{3}\right)^{1/2}\left((Z\sqrt{2}+1)\Gamma^{5/2}\ln\frac{k_{max}}{k_{min}}\right)^{-1}. \quad (14a)$$

For $Z=1$, Eq. (14) gives $D_2=1.70$ $D_2^{(1)}$, with $D_2^{(1)}$ evaluated through a one Sonine polynomial approximation. The argument under the logarithm in Eq. (14) documents the usual Coulomb logarithm $\sim\lambda_D/\lambda_L$ for $T\leq 1$ Ry, or $\lambda_D/\lambda_{DdB}$ for $T>1$ Ry. $\lambda_L$ denotes the usual Landau length $\lambda_L = e^2/k_B T$ and $\lambda_{DdB} = \hbar/\sqrt{2mk_B T}$, the electron De Broglie wavelength, taking care of the intrinsically quantum behav-
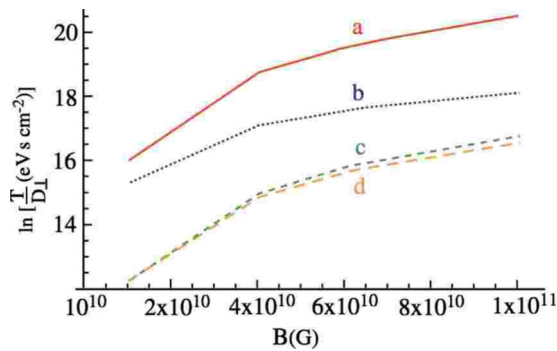


FIG. 2. (Color online) Proton transverse LIVSD in a dense target ($n=10^{21}$ $e$-cm$^{-3}$, $T=1$ keV) in terms of $B$ (G); (a) classical electron contribution to stopping, Eq. (9a); (b) Bohm-like electron contribution to stopping, Eq. (10); (c) classical ion contribution to stopping, Eq. (9a); (d) Bohm-like ion contribution to stopping, Eq. (10).
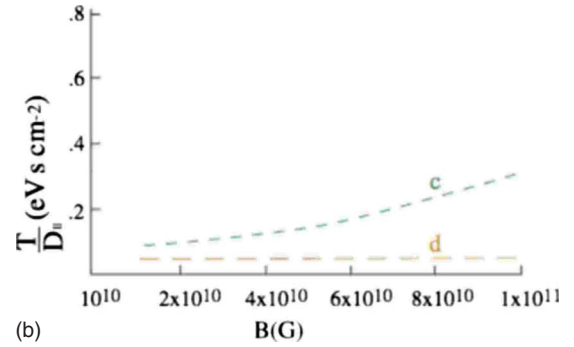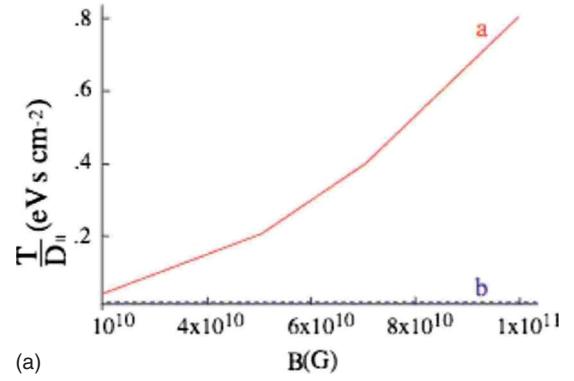




FIG. 3. (Color online) Proton parallel LIVSD in a dense target ($n=10^{21}$ $e$-cm$^{-3}$, $T=1$ keV) in terms of $B$ (G): (a) Bohm-like electron contribution to stopping, Eq. (11); (b) classical electron contribution to stopping, Eq. (9a); (c) Bohm-like ion contribution to stopping, Eq. (11); (d) classical ion contribution to stopping, Eq. (9a).

ior of the high-temperature plasma in the short range limit [23].

Finally, one has also to pay attention to the parallel diffusion coefficient (9a) featuring the $\omega_b \geq \omega_p$ range. The three given approaches are thus contrasted in Fig. 1 where curve (a) features Eqs. (12) and (13), curve (b) implements Eqs. (2)–(14), while curve (c) illustrates the same process through the $B$-independent diffusion coefficient (9a).

The rather handsome matching of the three independent approaches at $B=0$, in a dense but still weakly coupled target plasma, encourages us to investigate further the strongly magnetized ones.
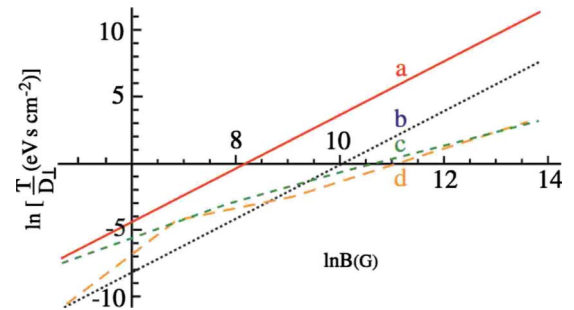


FIG. 4. (Color online) Proton transverse LIVSD in a cold plasma ($n=3.5\times10^7$ $e$-cm$^{-3}$, $T=100$ °K) in terms of $10^2\leq B$(G) $\leq 10^6$; (a) target electron slowing down ($D_\perp\sim B^{-2}$), Eq. (9b) (b) target ion slowing down ($D_\perp\sim B^{-2}$), Eq. (9b); (c) Target electron slowing down ($D_\perp\sim B^{-1}$), Eq. (10); (d) target ion slowing down ($D_\perp\sim B^{-1}$), Eq. (10).
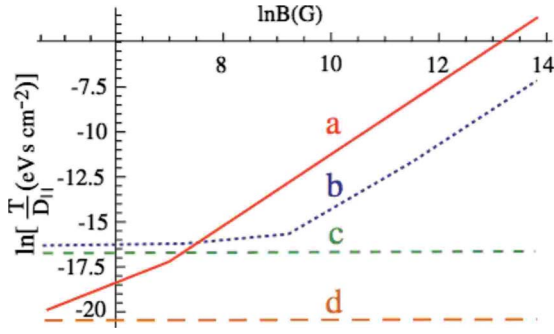
FIG. 5. (Color online) Proton parallel LIVSD in a cold plasma with $n = 3.5 \times 10^7$ $e$-cm$^{-3}$, $T = 100$ K in terms of magnetic intensity $10^2 \leqslant B$ (G) $\leqslant 10^6$: (a) target electron slowing down for $B \neq 0$, Eq. (11); (b) target ion slowing down for $B \neq 0$ Eq. (11); (c) target ion slowing down with $B$-independent $D$, Eq. (9a); (d) target electron slowing down with $B$-independent $D$, Eq. (9a).

## IV. LIVSD IN STRONGLY MAGNETIZED TARGETS

We are now ready to implement the DB expression (2) through the diffusion coefficients for strongly magnetized OCP [Eqs. (9a), (9b), (10), and (11)], we thus emphasis transverse and parallel LIVSD, which are quantities of great physical interest, but hardly accessible to the most sophisticated combinations of binary collision and dielectric approaches [2–5].
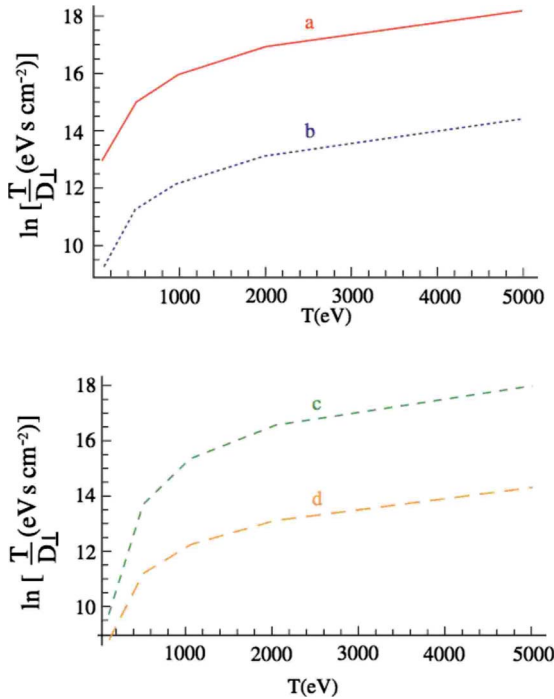


FIG. 6. (Color online) Proton transverse LIVSD in a dense plasma with $n = 10^{21}$ $e$-cm$^{-3}$, $100 \leqslant T$ (eV) $\leqslant 5000$ and $B = 10^{10}$ $G$ in terms of $T$ (eV): (a) target electron slowing down ($D_\perp \sim B^{-2}$), Eq. (9a); (b) target ion slowing down ($D_\perp \sim B^{-2}$), Eq. (9a); (c) target electron slowing down ($D_\perp \sim B^{-1}$), Eq. (10); (d) target ion slowing down ($D_\perp \sim B^{-1}$), Eq. (10).
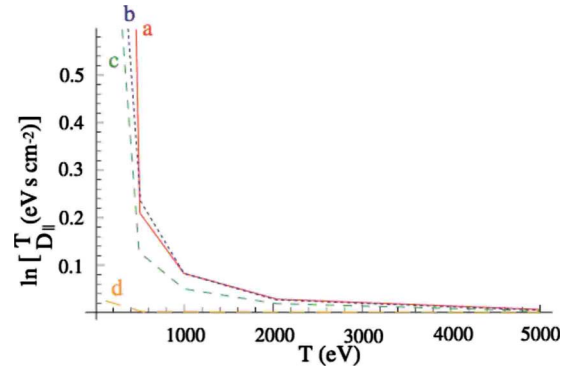


FIG. 7. (Color online) Proton parallel LIVSD in a dense plasma $n = 10^{21}$ $e$-cm$^{-3}$, $100 \leqslant T$ (eV) $\leqslant 5000$ and $B = 10^{10}$ G, in terms of $T$ (eV): (a) electron stopping ($B \neq 0$); (b) ion stopping ($B \neq 0$); (c) ion stopping ($B = 0$), (d) electron stopping ($B = 0$).

### A. *B* dependence

$D_\perp$ and $D_\parallel$ expressions introduced in Eq. (2) are expected to document a strong anisotropy between transverse and parallel slowing down. However, in both cases, $B$ dependence is obviously increasing with $B^2$ (classical) or $B$ (Bohmlike).

We thus consider respectively a dense and strongly magnetized target plasma envisioned for fast ignition in ICF [6–8] with $n = 10^{21}$ $e$-cm$^{-3}$, $T = 1$ keV and $10^{10} \leqslant B(G) < 10^{11}$ (see Figs. 2 and 3), and also a highly dilute ($n \sim 10^7$ $e$-cm$^{-3}$) one at very low temperature [$T(K) = 100$], (see Figs. 4 and 5 of current use for ion beam cooling [2–4,24], on the Lear accelerating line, at Cern for instance. In both cases, one witnesses a steady LIVSD increase with $B$, for both $D_\perp$ and $D\parallel$, when $B$ dependent $D$ expressions are introduced in Eq. (2).

### B. *T* dependence

The temperature behavior is much more intriguing, as respectively displayed on Figs. 6 and 7 for transverse and parallel LIVSD in the highly strongly magnetized and dense target already considered for fast ignition in ICF. One then witnesses a monotonous increase for transverse stopping
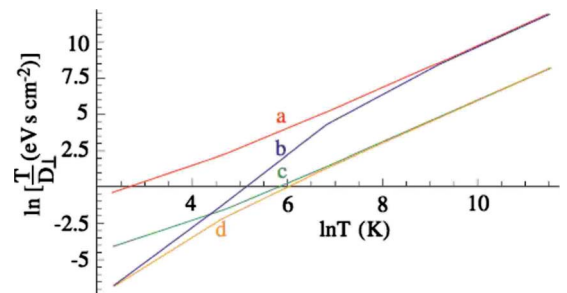


FIG. 8. (Color online) Proton transverse LIVSD in a cold plasma; $n = 3.5 \times 10^7$ $e$-cm$^{-3}$, $10 \leqslant T$ (K) $\leqslant 10^5$ and $B = 10^4$ G, in terms of $T$ (K); (a) target electron slowing down ($D_\perp \sim B^{-2}$). Eq. (9a); (b) target electron slowing ($D_\perp \sim B^{-1}$), Eq. (10); (c) target ion slowing down ($D_\perp \sim B^2$), Eq. (9a); (d) target ion slowing down ($D_\perp \sim B^{-2}$), Eq. (10).
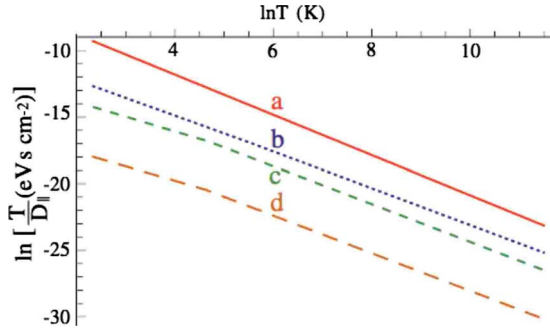
FIG. 9. (Color online) Proton parallel LIVSD in a cold plasma; $n=3.5\times10^7$ cm$^{-3}$, $B=10^4$ G), $10 \leqslant T$ (K) $\leqslant 10^5$; (a) target ion slowing down ($B\neq0$); (b) target ion slowing down ($B=0$); (c) target electron slowing down ($B\neq0$); (d) target electron slowing ($B=0$). (b) and (c) stand in a ln (43) ratio.



FIG. 10. (Color online) Proton transverse LIVSD in a dense plasma ($n=10^{21}$ $e$-cm$^{-3}$, $B=10^{10}$ G) in terms of temperature $T$ (eV) through target ion stopping: (a) Eq. (9b), (b) Eq. (15), and (c) Eq. (10).

(Fig. 6) contrasted to a monotonous decay for the parallel counterpart (Fig. 7).

Such a behavior is likely to be generic, because one retrieves it in the very different situation of the cold plasma used for ion beam cooling [2–4,24], as evidenced by the corresponding transverse (Fig. 8) and parallel (Fig. 9) behaviors.

The intermediate regime alluded to in Ref. [20], with $D_\perp \sim B^0$, corresponds to the diffusion coefficient [14],

$$D'_\perp = D_\perp^{(0)}\left(1 + \frac{0.6\varepsilon_p\nu_c}{r^2\omega_p}\right), \tag{15}$$

with the ensuing LIVSD pictured as curve (b) ion Fig. 10, dedicated to transverse slowing down in a dense target with $n=10^{21}$ $e$-cm$^{-3}$, $B=10^{10}$ G in terms of temperature. As anticipated, expression (15) yields LIVSD very close to those deduced from Eq. (9b).

## V. SUMMARIES

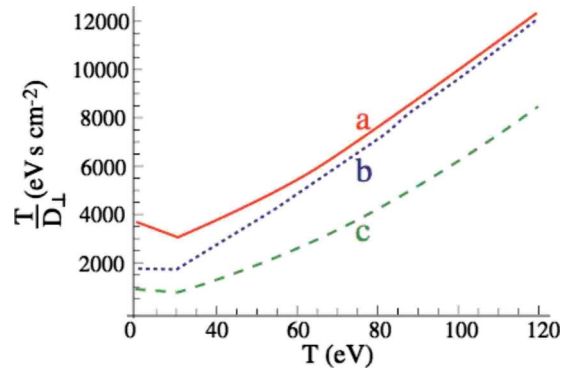As a summary, we implemented the very simple LIVSD expression (2) to the *a priori* very involved ion beam arbitrarily magnetized plasma interaction. We used transverse and parallel diffusion coefficients [14,15] in suitably framed magnetized one component plasma (OCP) with target electrons building up the corresponding neutralizing background. Thus we reached analytic LIVSD transverse and parallel expressions advocating contrasting temperature behaviors. These quantities are of obvious significance in asserting the confinement capabilities of a very large scope of dense and strongly magnetized plasmas ranging from ultracold ones [1] to those featuring the highest $B$ values one can produce in the laboratory or observe in astrophysics [2–9].

It should also be appreciated that in contradistinction to the usual perturbative techniques of current use [2–5], our present asymptotic analysis produces analytic LIVSD expressions, which are of immediate use for numerical coding.

[1] T. C. Killian, Science **316**, 705 (2007).

[2] H. Nersisyan, C. Toepffer, and G. Zwicknagel, *Interaction Between Charged Particles in a Magnetic Field* (Springer-Verlag, Berlin, 2007).

[3] H. B. Nersisyan, M. Walter, and G. Zwicknagel, Phys. Rev. E **61**, 7022 (2000); H. B. Nersisyan, G. Zwicknagel, and C. Toepffer, *ibid.* **67**, 026411 (2003).

[4] C. Toepffer, Phys. Rev. A **66**, 022714 (2002); B. Möllers, M. Walter, G. Zwicknagel, C. Carli, and C. Toepffer, Nucl. Instrum. Methods Phys. Res. B **207**, 462 (2003).

[5] C. Cereceda, C. Deutsch, M. DePeretti, M. Sabatier, and H. B. Nersisyan, Phys. Plasmas **7**, 2884 (2000); C. Cereceda, M. DePeretti, and C. Deutsch, *ibid.* **12**, 022102 (2005).

[6] M. Tabak, J. Hammer, M. E. Glinsky, W. L. Kruer, S. C. Wilks, J. Woodworth, E. M. Campbell, M. D. Perry, and R. J.

Mason, Phys. Plasmas **1**, 1626 (1994); C. Deutsch, H. Furukawa, K. Mima, M. Murakami, and K. Nishihara, Phys. Rev. Lett. **77**, 2483 (1996).

[7] M. Roth, T. E. Cowan, M. H. Key, S. P. Hatchett, C. Brown, W. Fountain, J. Johnson, D. M. Pennington, R. A. Snavely, S. C. Wilks, K. Yasuike, H. Ruhl, F. Pegoraro, S. V. Bulanov, E. M. Campbell, M. D. Perry, and H. Powell, Phys. Rev. Lett. **86**, 436 (2001); C. Deutsch, Eur. Phys. J.: Appl. Phys. **24**, 95 (2003).

[8] See, for instance, M. Tatarakis, F. N. Beg, E. L. Clark, A. E. Dangor, R. D. Edwards, R. G. Evans, T. J. Goldsack, K. W. D. Ledingham, P. A. Norreys, M. A. Sinclair, M-S. Wei, M. Zepf, and K. Krushelnick, Phys. Rev. Lett. **90**, 175001 (2003).

[9] D. Winske and S. Peter Gary, J. Geophys. Res. **112**, A10303 (2007).

[10] J. W. Dufty and M. Berkovsky, Nucl. Instrum. Methods Phys. Res. B **96**, 626 (1995); J. W. Dufty, B. Talin, and A. Calisti, Adv. Quantum Chem. **46**, 293 (2004).

[11] H. Paul and A. Schinner, Nucl. Instrum. Methods Phys. Res. B **227**, 461 (2000).

[12] C. Deutsch, Ann. Phys. (Paris) **11**, 1 (1986); C. Deutsch and G. Maynard, Recent Res. Devel. Plasmas **1**, 1 (2000).

[13] A fundamental restriction on the relations (2) arises *a priori* from the strong inequality $Mp/m \geqslant 1$ between ion projectile and electron mass. However, Dufty and Berkovsky [10] demonstrate how it can be considerably relaxed.

[14] M. C. Marchetti, T. R. Kirkpatrick, and J. R. Dorfman, J. Stat. Phys. **46**, 679 (1987); **49**, 871 (1987); Phys. Rev. A **29**, 2960 (1984).

[15] J. S. Cohen and L. G. Suttorp, Physica A **126**, 308 (1984).

[16] The extension to a more general ion beam-plasma system requires us to replace the OCP by a binary ionic mixture (BIM) modelization.

[17] R. J. Goldston and P. H. Rutherford, *Introduction to Plasma Physics* (Institute of Physics, Philadelphia, 1995), p. 198.

[18] D. Montgomery, C. S. Liu, and G. Vahala, Phys. Fluids **15**, 815 (1972).

[19] M. Steinberg and J. Ortner, Phys. Rev. E **63**, 046401 (2001).

[20] It could be appreciated that switching from the classical expression (9b) to the hydrodynamic Bohmlike (10) we overlooked the intermediate regime with $D_\perp \sim 1/B^0$ as evidenced, for instance, in H. Okuda and J. M. Dawson, Phys. Rev. Lett. **28**, 1625 (1972). The reason is that numerically when introduced in Eq. (2), the corresponding LIVSD results are hardly distinguishable from classical ones [Eq. (9b)] as shown in Sec. V.

[21] T. Peter and J. Meyer-ter-Vehn, Phys. Rev. A **43**, 1998 (1991).

[22] L. Sjögren, J. P. Hansen, and E. L. Pollock, Phys. Rev. A **24**, 1544 (1981).

[23] C. Deutsch, Phys. Lett. A **60**, 317 (1977).

[24] G. Zwicknagel, in *Electron Cooling of Ions and Antiprotons in Traps*, edited by S. Nagaitsev and R. J. Pasquinelli, AIP Conf. Proc. No. 821 (AIP, Melville, NY, 2006), pp. 513–522.